Scattering from Two-Dimensional Objects of Varying Shape Combining the Method of Moments with the Stochastic Galerkin Method

Zdravko Zubac[1], Daniel De Zutter[1], Dries Vande Ginste[1]

***Abstract*—In this communication, the Combined Field Integral Equation for perfect electrically conducting scatterers is combined with the Stochastic Galerkin Method (SGM) to model the impact of stochastic variations of the shape of the scatterer on the radar cross-section and on the induced current distribution. The SGM is compared to the Stochastic Collocation Method (SCM) and it is shown that for a modest number of random variables the SGM is a good alternative to the SCM.**

***Index Terms*—Stochastic Galerkin Method (SGM), Stochastic Collocation method (SCM), scattering, Method of Moments (MoM)**

I. Introduction

Electromagnetic solvers are widely used in the analysis of scattering and remote sensing problems as well as in the analysis and design of antennas and high-speed systems, to model electromagnetic compatibility problems and in many other domains. The straightforward way to assess the influence of geometrical or material variations and uncertainties with these solvers is by implementing Monte Carlo (MC) simulations. The major drawback of MC is the slow convergence at a rate of $1/\sqrt{n}$, where n is the number of separate runs of the code. More sophisticated methods have been proposed based on the expansion of the quantities of interest into a (truncated) polynomial chaos expansion (PCE) using orthogonal polynomials depending on the particular distribution of the random variables [1]. These methods come in two flavors: the non-intrusive Stochastic Collocation Method (SCM) [2] and the intrusive Stochastic Galerkin Method (SGM) [3]. PCE-based methods are already used for variability analysis of (on-chip) interconnects [4] [5] [6]. Very recently, polynomial chaos was introduced in the Finite Difference Time Domain (FDTD) analysis of microwave circuits [7]. Furthermore, a thorough discussion of the use of a PCE-method, more particularly a multi-element SCM, for statistical EMC/EMI characterization, was presented in [8]. Calculation of the statistical properties of two-dimensional electromagnetic scattering from random rough surfaces combining the MC approach with a deterministic method of moments simulator is discussed in [9]. In view of the superiority of PCE-based methods over MC simulations, [10] presents the combination of the SCM with a time-domain Finite Element technique for scattering by two- and three-dimensional perfectly electrically conducting objects of varying shape.

In view of previous work, in particular [8], this paper focusses on the use of the SGM as compared to the SCM to model stochastic scattering problems by means of integral equations and the Method of Moments (MoM). To the best knowledge of the authors, this communication is the first to discuss the SGM-MoM combination for scattering problems. We restrict ourselves to frequency domain scattering by two-dimensional PEC objects under TM-incidence to keep this communication sufficiently succinct. In order to see what the benefits and drawbacks of SGM are compared to SCM, of course we also provide the necessary numerical data to compare both approaches. Furthermore, we do not only present results for the radar cross-section, but also pay attention to the current distribution on the scatterer.

Section II first briefly introduces the combined field integral equation and its MoM discretization. Next, a discussion is provided on the polynomial chaos expansion in the MoM, with particular emphasis on the differences between SGM and SCM. In Section III, two pertinent examples are discussed in detail. In these examples we consider different distributions: uniform and uncorrelated in the first example and correlated with a Gaussian covariance matrix in the second example. Conclusions are formulated in Section IV.

II. The stochastic scattering problem

We consider two-dimensional frequency domain scattering by PEC objects, residing in free space, the geometry of which is not deterministic but varies stochastically. The z-axis is the axis of invariance. The incident wave is a TM-polarized plane wave with electric field $\boldsymbol{E}^i = E^i \mathbf{u}_z$. The $e^{j\omega t}$-dependence is suppressed. To determine the scattered field, we apply a surface integral equation technique. Although the electrical field integral equation (EFIE) can be used for both open and closed structures, the combined field integral equation (CFIE) is preferred for closed structures to avoid spurious resonances. For brevity, we assume that the reader is familiar with the CFIE. This integral equation can be solved by the MoM. N pulse basis functions $b_j, j = 1, 2, ..., N$, are introduced to expand the unknown surface current density J_z on the PEC scatterer as:

$$J_z(\boldsymbol{\rho}') = \sum_{j=1}^{N} I_j b_j(\boldsymbol{\rho}'), \tag{1}$$

with I_j the unknown expansion coefficients. Applying a Galerkin testing procedure then yields a $N \times N$ linear system in the unknown expansion coefficients I_j:

$$\sum_{j=1}^{N} Z_{ij} I_j = V_i, \quad i = 1, 2, ..., N \qquad \text{or} \qquad \overline{\boldsymbol{Z}}\boldsymbol{I} = \boldsymbol{V}. \tag{2}$$

We do not give the explicit expressions for $\overline{\boldsymbol{Z}}$ and $\boldsymbol{V}$ as the readers are undoubtedly familiar with them. Now suppose the scatterer is not defined deterministically but has a geometry which exhibits some inherent variability. This variability is described by a set of M random variables. We assume that these variables are independent random variables which are collected in the vector $\boldsymbol{\xi} = [\xi_1\ \xi_2\ ...\ \xi_M]$. The case of correlated variables can be treated as well by starting from a properly defined set of independent variables or, for Gaussian random variables, by adopting a Karhunen-Loève transformation (KLT) [11]. All quantities in (2) now depend on $\boldsymbol{\xi}$, i.e:

$$\overline{\boldsymbol{Z}}(\boldsymbol{\xi})\boldsymbol{I}(\boldsymbol{\xi}) = \boldsymbol{V}(\boldsymbol{\xi}). \tag{3}$$

[1]Electromagnetics Group, Department of Information Technology, Ghent University, Sint-Pietersnieuwstraat 41, 9000 B-Gent, Belgium. E-mail: zdravko.zubac@UGent.be. This work has been funded by the Interuniversity Attraction Poles Programme initiated by the Belgian Science Policy Office.

The goal of solving (3) is to determine the full statistics of the induced currents, of the scattered fields, and in particular of the radar cross-section (RCS). To this end, all quantities of interest are represented in terms of a truncated polynomial chaos expansion

$$Z_{ij}(\boldsymbol{\xi}) = \sum_{k=0}^{K} Z_{ij,k}\phi_k(\boldsymbol{\xi}), \qquad (4a)$$

$$V_i(\boldsymbol{\xi}) = \sum_{k=0}^{K} V_{i,k}\phi_k(\boldsymbol{\xi}), \qquad I_j(\boldsymbol{\xi}) = \sum_{k=0}^{K} I_{j,k}\phi_k(\boldsymbol{\xi}), \qquad (4b)$$

where $Z_{ij,k}$, $V_{i,k}$ and $I_{j,k}$ are expansion coefficients and the $\phi_k(\boldsymbol{\xi})$ are multivariate polynomials that are orthonormal with respect to the probabilistic density functions relevant to the particular scattering problem that is treated. Hence, $< \phi_j(\boldsymbol{\xi}), \phi_k(\boldsymbol{\xi}) >= \delta_{jk}$, with the inner product $< f(\boldsymbol{\xi}), g(\boldsymbol{\xi}) >$ defined as

$$< f(\boldsymbol{\xi}), g(\boldsymbol{\xi}) >= \int_{\xi_1} \cdots \int_{\xi_M} f(\boldsymbol{\xi}) g(\boldsymbol{\xi}) W(\boldsymbol{\xi}) d\xi_1 \cdots d\xi_M \qquad (5)$$

and with $\delta_{jk} = 0$ for $j \neq k$ and $\delta_{jk} = 1$ for $j = k$. $W(\boldsymbol{\xi})$ is the probability density function associated with the random vector $\boldsymbol{\xi}$. As we work with independent stochastic variables, W is the product of the probability density functions $W_m, m = 1, 2, .., M$, of the individual random variables ξ_m. The polynomials $\phi_k(\boldsymbol{\xi})$ themselves are constructed as products of univariate polynomials only depending on a single random variable. For each multivariate polynomial, the *total degree*, i.e. the sum of the orders of the univariate polynomials, is at most P. This maximum order is a parameter that we can choose. The number M of random variables determines the number $K + 1$ of multivariate polynomials as follows:

$$K + 1 = \frac{(M + P)!}{M!P!}. \qquad (6)$$

$Z_{ij,k}$ and $V_{i,k}$ in (4) are obtained through projection:

$$V_{i,k} =< V_i(\boldsymbol{\xi}), \phi_k(\boldsymbol{\xi}) >, \quad Z_{ij,k} =< Z_{ij}(\boldsymbol{\xi}), \phi_k(\boldsymbol{\xi}) > . \qquad (7)$$

By substituting (4) into (2), we get

$$\sum_{k=0}^{K} V_{i,k}\phi_k(\boldsymbol{\xi}) = \sum_{j=1}^{N}\sum_{k=0}^{K}\sum_{l=0}^{K} Z_{ij,k} I_{j,l}\phi_k(\boldsymbol{\xi})\phi_l(\boldsymbol{\xi}), \qquad \forall\, i. \qquad (8)$$

Galerkin projection of both sides of (8) on ϕ_m finally leads to the following set of equations for the $I_{j,k}$ in (4b)

$$\tilde{\boldsymbol{V}} = \tilde{\overline{\boldsymbol{Z}}}\tilde{\boldsymbol{I}}, \qquad (9)$$

where $\tilde{\overline{\boldsymbol{Z}}}$ is a deterministic matrix given by

$$\tilde{\overline{\boldsymbol{Z}}} = \sum_{k=0}^{K} \left(\begin{pmatrix} \gamma_{k00} & \gamma_{k10} & \cdots & \gamma_{kK0} \\ \gamma_{k01} & \gamma_{k11} & \cdots & \gamma_{kK1} \\ \vdots & \vdots & \ddots & \vdots \\ \gamma_{k0K} & \gamma_{k1K} & \cdots & \gamma_{kKK} \end{pmatrix} \otimes \overline{\boldsymbol{Z}}_k \right), \qquad (10)$$

with $\gamma_{klm} =< \phi_k(\boldsymbol{\xi})\phi_l(\boldsymbol{\xi}), \phi_m(\boldsymbol{\xi}) >$ and where $\otimes$ stands for the Kronecker product of matrices. The $N \times N$ matrix $\overline{\boldsymbol{Z}}_k$ is similar to $\overline{\boldsymbol{Z}}$ in (2), but with the Z_{ij} replaced by $Z_{ij,k}$; $\tilde{\boldsymbol{V}}^T = [V_{1,0}...V_{N,0}V_{1,1}...V_{N,1}...V_{1,K}...V_{N,K}]$ and similarly for $\tilde{\boldsymbol{I}}$. Eqn. (10) shows that the application of the SGM leads to a new system matrix the size of which is now much larger, i.e. $(K + 1)N \times (K + 1)N$ instead of $N \times N$. However, this new system is deterministic, as thanks to the Galerkin projection the dependence on $\boldsymbol{\xi}$ has vanished. Solving (9) yields $\tilde{\boldsymbol{I}}$. Inserting this solution into (4b) then yields the full statistics of the induced current. For example, the mean value of this current on the j-th segment ($j = 1, 2, ..., N$) is given by

$$\mathrm{E}[I_j(\boldsymbol{\xi})] = I_{j,0}, \qquad (11)$$

where $\mathrm{E}[\cdot]$ denotes the expected value operator. The variance is computed as

$$\mathrm{E}[|I_j(\boldsymbol{\xi}) - \mathrm{E}[I_j(\boldsymbol{\xi})]|^2] = \sum_{k=1}^{K} |I_{j,k}|^2. \qquad (12)$$

Besides the above stochastic moments, the probability density functions (PDF) and cumulative distribution functions (CDF) can also be readily computed from (4).

Obviously, the SGM, presented above, is an intrusive method. The Stochastic Collocation Method (SCM) is non-intrusive. We refer the reader to [8] for details. In the SCM any quantity of interest $f(\boldsymbol{\xi})$ is expanded as:

$$f(\boldsymbol{\xi}) = \sum_{k=0}^{K} f_k\phi_k(\boldsymbol{\xi}), \qquad (13a)$$

$$f_k =< f(\boldsymbol{\xi}), \phi_k(\boldsymbol{\xi}) >\approx \sum_{r=1}^{N_p} w_r f(\boldsymbol{\xi}_r)\phi_k(\boldsymbol{\xi}_r), \qquad (13b)$$

where w_r and $\boldsymbol{\xi}_r$ are the weights and sampling points of the quadrature. Consequently, in the SCM, the desired statistical information is obtained by knowledge of the solution of (3) in N_p sampling points in the M-dimensional space of the random variables $\boldsymbol{\xi}$. The SCM can thus easily be built on top of a deterministic code by solving N_p deterministic problems (2).

III. Numerical examples.

A. Scattering by a finite periodic array of PEC strips

As a first example, consider TM-scattering by a periodic but finite array of five PEC strips as depicted in Fig. 1. The x-coordinates of the position vectors of the centers of the strips remain fixed with constant spacing T. However, the widths of the strips w and their heights h w.r.t. a nominal plane are chosen to be independent uniformly distributed random variables, hence $M = 10$. The widths of the strips vary between $0.2T$ and $0.8T$, with $T = 3\lambda/4$, and the heights of the strips between $-\lambda/10$ and $\lambda/10$, where λ is the wavelength of the incident wave. In the MoM analysis, the discretization of each strip will be chosen fine enough and such that the number of divisions remains identical when considering varying widths.

As uniform distributions are considered, normalized Legendre polynomials are the appropriate functions to model the uncertainty. This implies that in (5), the multivariate polynomials $\phi_j(\boldsymbol{\xi})$ are constructed as products of univariate Legendre polynomials. When calculating the matrix elements

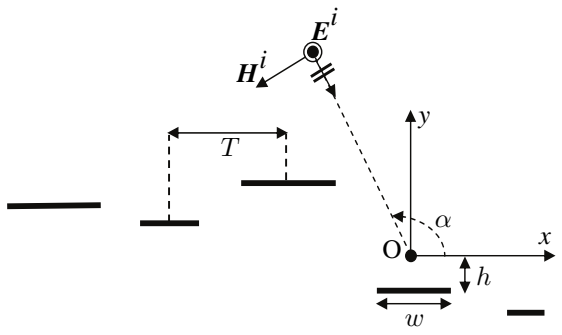

Fig. 1. Periodic array of PEC strips. Widths w and heights h are random.

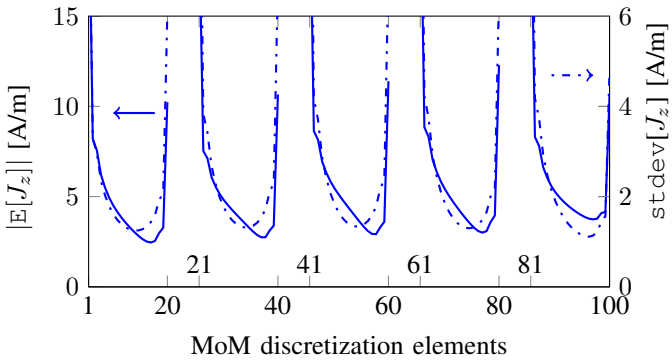

Fig. 2. Magnitude of the mean value (full line) and standard deviation (dash-dotted line), of the current distribution for total degree $P = 4$ for the example of Fig. 1.

in (3) or (9), elements describing MoM interactions on the same strip only depend on a single random variable, i.e. the width, and all other matrix elements depend on four random variables, the two heights and the two widths. The right hand side data depend on two random variables. The incident wave is a TM-polarized plane wave impinging under an angle $\alpha = 3\pi/4$ with the positive x-axis.

The current on each of the five strips is modeled using 20 equal length subdivisions on which the current is taken to be constant, i.e. the total number of unknowns in the MoM is $N = 100$. For this example and the following ones, the quantities of interest (surface current, RCS, impedance matrix elements) are modeled using expansions of type (13a) with highest polynomial order, i.e. total degree, $P = 4$. Our experience shows that $P = 4$ suffices to accurately describe the wanted statistics. To assess the effect of this total degree, below, results for $P = 4$ will be compared to results for $P = 1$, $P = 2$ and $P = 3$. Due to the fact that calculating the expansion coefficients according to (13b) implies that, for $P = 4$, up to eight-order polynomials play a role, we opt for an integration scheme that assures correct integration up to and including order 9. When lowering the total degree P, we lower the accuracy of the integration scheme at the same time, as such using the most optimal approach.

Both in SGM and in SCM we have to calculate integrals of the form (13b) to obtain the expansion coefficients of the quantities of interest. In the present example, these integrals are integrals over a 10-dimensional parameter space. Naive application of Gauss-Legendre quadrature with 5 sampling points (to assure exact integration for polynomials up to order 9) leads to $N_p = 5^{10}$ sampling points in (13b). This huge number can however be avoided by applying Smolyak's rule. Smolyak's rule or Smolyak integration is a sparse grid technique to integrate high dimensional functions [12]. This particular sparse grid technique only requires $N_p = 8761$ sampling points for about the same accuracy, i.e. a reduction by more than a factor of 1000. For smaller values of P, even less Smolyak points are needed: $N_p = 21$ for $P = 1$, $N_p = 221$ for $P = 2$ and $N_p = 1581$ for $P = 3$.

From (6), including multivariate polynomials up to total degree $P = 4$ in SGM, implies that $K + 1 = 1001$. To find the $Z_{ij,k}$ in (8), Smolyak's rule requires $N_p \times N^2$ interaction integrals to be calculated followed by the solution of a *single* linear system (9) of dimension $(K + 1)N \times (K + 1)N$.

On the other hand, applying SCM again consists in calculating $N_p \times N^2$ MoM interaction integrals and the solution of not a single but of N_p linear systems of size $N \times N$. It is immediately clear that straightforward application of SGM leads to a numerical effort which vastly exceeds that of SCM. However, the purpose of the present example is to demonstrate that the above conclusion is not necessarily unavoidable when taking the particular nature of the considered problem into account. Indeed, remark that the Z_{ij} only depend on the width, when considering interactions on the *same* strip. For strip to strip interactions only four variables matter. Thus, in SGM, we do not need to consider the full ten-dimensional parameter space and this has a very considerable impact on the CPU-time as will become clear from the numerical results.

Before turning to these numerical results, let us also point out the following. Iteratively solving the large linear system (9) not only requires a lot of CPU-time but storing all matrix elements can lead to very high (or even impossibly high) memory requirements. To alleviate this problem, we only store the $Z_{ij,k}$ of matrix $\overline{\boldsymbol{Z}}_k$ in (10). It so turns out that quite a large number of the γ_{klm} also needed in (10) are zero. The non-zero ones can easily be stored and the Kronecker product is then calculated on-the-fly when iteratively solving (9).

For $P = 4$, Fig. 2 shows the magnitude of the mean value $|\mathrm{E}(J_z)|$ (11) and the standard deviation (stdev) of the induced current, i.e. the square root of the variance defined in (12). Results for SGM, SCM and MC are indistinguishable on the scale of the figure. For both SGM and SGM, CPU-time and memory requirements are given in Table I as a function of P, together with the mean value and variance of the absolute value of the center current on subdivision 10. For this particular example, the MC analysis was performed using 5×10^4 samples. The values obtained with SCM and SGM clearly converge to the same value, while the MC result has not yet converged to this value. In this example, SGM remains more CPU-time efficient than SCM up to $P = 3$.

The radar cross-section (RCS) is given by

$$\sigma_{2D} = \lim_{\rho \to \infty} 2\pi\rho \frac{|E_z^s|^2}{|E_z^i|^2}, \tag{14}$$

where ρ is the distance to the origin O in Fig. 1, E_z^i is the incident electric field and E_z^s is the scattered electric

TABLE I
SIMULATION DATA FOR THE PEC STRIP ARRAY

method	P	memory	CPU-time	mean	variance
SGM	1	1.7 MB	3.8 s	3.5420	1.6726
SGM	2	10.3 MB	34.8 s	3.5527	1.7034
SGM	3	45.7 MB	290 s	3.5376	1.7177
SGM	4	172 MB	50 m	3.5369	1.7227
SCM	1	50 kB	5 s	3.5476	1.4366
SCM	2	403 kB	56 s	3.5319	1.6872
SCM	3	4.8 MB	394 s	3.5376	1.7258
SCM	4	71 MB	37 m	3.5370	1.7279
MC 5×10^4	-	-	3 h 30 m	3.5381	1.7242

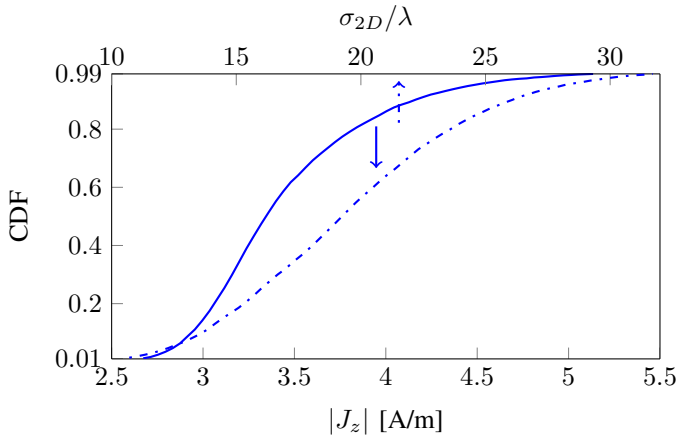

Fig. 3. CDF for the amplitude of the current for the 10th MoM subdivision (full line) and for the RCS in the direction of specular reflection (dash-dotted line) for the example of Fig. 1.

field which can be derived from the induced currents. Fig. 3 shows both the Cumulative Distribution Function (CDF) of the absolute value of the current induced on subdivision 10 and the CDF of the RCS in the specular reflection direction, i.e. in the direction making an angle of $\pi/4$ with the x-axis. Remark that both quantities vary considerably over the space of random variables. In order to correctly represent the relative behavior of the two CDFs, the minimum and maximum values on the horizontal axes for both current and RCS correspond to CDF-values of 0.01 and 0.99 respectively.

B. Non-smooth surface

As a second example consider the TM-scattering by a non-smooth finite PEC-strip of width w (see Fig. 4). The roughness of this strip is described by a stochastic Gaussian process. To this end the strip is divided in $M-1$ segments. The x-coordinates of the endpoints of each segment remain fixed and are equidistantly spaced, i.e. $\Delta x = w/(M-1)$. However, the corresponding y-coordinates are situated at a variable positive or negative height above a reference level, as also indicated on Fig. 4. We collect these y-coordinates in a height vector $\boldsymbol{h} = [y_1\ y_2\ ...\ y_M]^T$. The roughness is described by the following stochastic Gaussian process

$$P(\boldsymbol{h}) = \frac{1}{\sqrt[M]{2\pi}} e^{-\frac{1}{2}\boldsymbol{h}^T \overline{\boldsymbol{\Sigma}}^{-1} \boldsymbol{h}} \tag{15}$$

and a Gaussian correlation matrix the elements of which are

$$[\overline{\boldsymbol{\Sigma}}(\boldsymbol{r})]_{ij} = \sigma^2 e^{-\frac{|\boldsymbol{r}_i - \boldsymbol{r}_j|^2}{L_c^2}} \tag{16}$$

where L_c is the correlation length, σ the standard deviation and with $\boldsymbol{r}_j$ the position vector of each endpoint, i.e. $\boldsymbol{r}_j = x_j \boldsymbol{u}_x + y_j \boldsymbol{u}_y$. The dimension of the random space considered in this example is M. The correlated random variables are decorrelated by means of the KLT. First, the correlation matrix is diagonalized:

$$\overline{\boldsymbol{U}}^T \overline{\boldsymbol{\Sigma}}\, \overline{\boldsymbol{U}} = \overline{\boldsymbol{\Lambda}}. \tag{17}$$

Second, the random heights $\boldsymbol{h}$ are described in terms of a set of M independent *standard normal* random variables $\boldsymbol{\xi} = [\xi_1\ ...\ \xi_M]$ through

$$\boldsymbol{h} = \mathrm{E}[\boldsymbol{h}] + \overline{\boldsymbol{U}}\, \overline{\boldsymbol{\Lambda}}^{1/2}\, \boldsymbol{\xi} \tag{18}$$

where $\mathrm{E}[\boldsymbol{h}]$ is the mean value of random vector $\boldsymbol{h}$. In this case, the appropriate polynomials to model the uncertainty are orthonormalized Hermite polynomials. The incident wave is

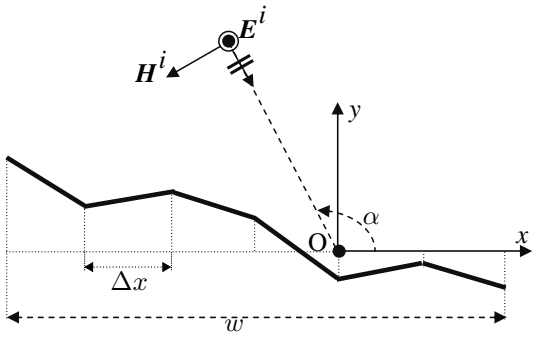

Fig. 4. Non-smooth PEC surface described by a set of points with variable height w.r.t. a reference plane.

identical to the one used in the previous example except for the angle of incidence which is now $\alpha = 2\pi/3$.

The numerical results discussed below are for a strip with width $w = 2\lambda$. The roughness of this strip is modeled with $M = 10$ Gaussian correlated random height variables with standard deviation $\sigma = \lambda/30$ and correlation length $L_c = \lambda/3$ in (16). For $M = 10$, the strip is modeled by 9 straight segments and 20 elementary unknowns per segment are introduced for the MoM, i.e., $N = 180$. We again compare SCM and SGM results and complement them by a MC analysis based on 5×10^4 samples.

Fig. 5 displays the magnitude of the mean value and the standard deviation of the current on each of the 180 MoM subdivisions. All simulation results are collected in Table II. The mean value and variance data are for the absolute value of the current near the center (MoM subdivision 90). Remark the excellent agreement between SGM and SCM, while, again, MC has not yet converged to yield correspondingly accurate results. For $P = 1$ and $P = 2$ the CPU-time needed, differs little, but the difference rapidly increases with P. Similar to Fig. 3, Fig. 6 shows the CDF of the absolute value of the current induced on subdivision 90 and the CDF of the RCS in the specular reflection direction, i.e. in the direction making an angle of $\pi/3$ with the x-axis.

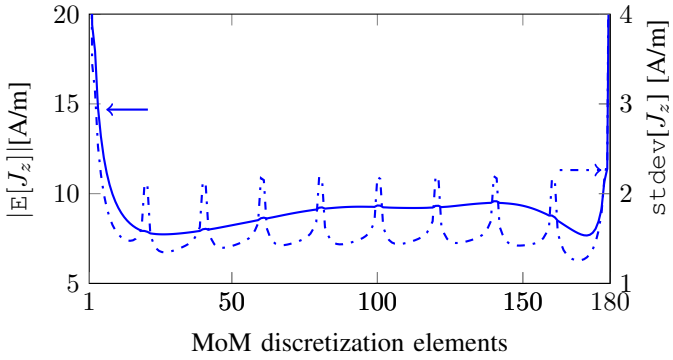

Fig. 5. Magnitude of the mean value (full line) and standard deviation (dash-dotted line), of the current distribution for the maximum polynomial order 4 for the example of Fig. 4

TABLE II
SIMULATION DATA FOR THE NON-SMOOTH SURFACE

method	P	memory	CPU-time	mean	variance
SGM	1	571 kB	17.8 s	9.2598	2.1054
SGM	2	28.2 MB	5.4 m	9.2615	2.0962
SGM	3	33.4 MB	37.4 m	9.2614	2.0969
SGM	4	460 MB	12 h	9.2614	2.0969
SCM	1	63.8 kB	17.2 s	9.2587	2.1436
SCM	2	486 kB	3 m	9.2615	2.0970
SCM	3	5 MB	21.8 m	9.2614	2.0970
SCM	4	56 MB	2 h 2 m	9.2614	2.0969
MC 5×10^4	-	-	11 h 10 m	9.2642	2.0954

IV. Conclusion

In this communication, we have shown how a frequency domain integral equation for scattering by two-dimensional PEC objects in free space can be combined with the intrusive Stochastic Galerkin Method. Attention is paid to the full statistics of the induced currents and the RCS due to stochastic changes in the geometry of the scatterer. The obtained results are compared to those of the non-intrusive stochastic collocation method which has already been studied in detail in literature. When applying the MoM with N unknowns, the CPU-time required by the SGM is dominated by the $(K+1)N \times (K+1)N$ deterministic matrix problem that has to be solved, where K is the number of multivariate polynomial chaos expansion polynomials. This number rapidly grows with the number of stochastic variables (the so-called curse of dimensionality) and also with the total degree P of the multivariate expansion polynomials. The CPU-time of the SCM is roughly proportional to N_p times solving an $N \times N$ system, with N_p the number of integration points needed to calculate expansion coefficients in the high- dimensional space of the stochastic variables. The two selected examples (with 10 random variables) show that up to total degree $P = 2$ both SCM and SGM remain comparable in CPU-time requirements. From $P = 3$ on, the SCM clearly becomes more efficient. For problems with a large number of stochastic variables, SCM is the only viable option.

From the numerical results (for the presented examples and several other ones), it also follows that it is very difficult to predict when a predefined accuracy has been reached, especially so for the variance. At present a mathematical criterion predicting the accuracy of the polynomial chaos expansion is lacking. Hence, from an engineering point of view, the best approach seems to be to start calculations with a low total degree P and with the minimum number of integration points needed for that degree. Increasing the total degree and the number of integration points should then reveal how trustworthy the as yet obtained data are.

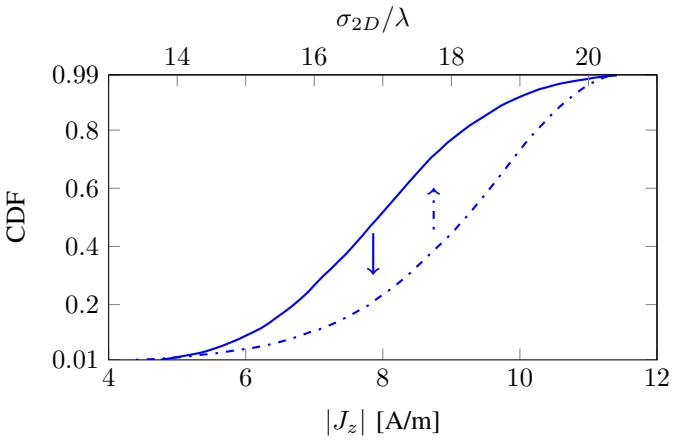

Fig. 6. CDF for the amplitude of the current for the 90th MoM subdivision (full line) and for the RCS in the direction of specular reflection (dash-dotted line) for the example of Fig.4

References

[1] D. B. Xiu and G. E. Karniadakis, "The Wiener-Askey polynomial chaos for stochastic differential equations," *SIAM Journal on Scientific Computing*, vol. 24, no. 2, pp. 619–644, 2002.

[2] D. Xiu, "Efficient collocational approach for parametric uncertainty analysis," *Communications in Computational Physics*, vol. 2, no. 2, pp. 293–309, Apr. 2007.

[3] R. G. Ghanem and P. D. Spanos, *Stochastic Finite Elements. A Spectral Approach*. New York:Springer-Verlag, 1991.

[4] D. Vande Ginste, D. De Zutter, D. Deschrijver, T. Dhaene, P. Manfredi, and F. Canavero, "Stochastic modeling-based variability analysis of on-chip interconnects," *IEEE Transactions on Components, Packaging and Manufacturing Technology*, vol. 2, no. 7, pp. 1182–1192, Jul. 2012.

[5] T. El-Moselhy and L. Daniel, "Variation-aware stochastic extraction with large parameter dimensionality: Review and comparison of state of the art intrusive and non-intrusive technique," in *2011 12th International Symposium on Quality Electronic Design (ISQED 2011), 14-16 March 2011, Santa Clara, CA, USA*, 2011, pp. 508–517.

[6] ——, "Stochastic extraction for SoC and SiP interconnect with variability," in *2011 IEEE Electrical Design of Advanced Packaging and Systems Symposium (EDAPS)*, 2011, pp. 1–4.

[7] A. Austin and C. Sarris, "Efficient analysis of geometrical uncertainty in the FDTD method using polynomial chaos with application to microwave circuits," *IEEE Transaction on Microwave Theory and Techniques*, vol. 61, no. 12, pp. 4293–4301, Dec. 2013.

[8] A. Yücel, H. Bağci, and E. Michielssen, "An adaptive multi-element probabilistic collocation method for statistical EMC/EMI chracterization," *IEEE Transaction on Electromagnetic Compatibility*, vol. 55, no. 6, pp. 1154–1168, Dec. 2013.

[9] R. L. Wagner, J. M. Song, and W. Chew, "Monte Carlo simulation of electromagnetic scattering from two-dimensional random rough surfaces," *IEEE Transactions on Antennas and Propagtion*, vol. 45, no. 2, pp. 235–245, Feb. 1997.

[10] C. Chauvière, J. S. Hesthaven, and L. C. Wilcox, "Efficient computation of RCS from scatterers of uncertain shapes," *IEEE Transactions on Antennas and Propagation*, vol. 55, no. 5, pp. 1437–1448, May 2007.

[11] M. Loeve, *Probability Theory II*. Springer, 1994.

[12] S. Smolyak, "Quadrature and interpolation formulas for tensor products of certain classes of functions," *Doklady Akademii Nauk SSSR*, vol. 4, pp. 240–243, 1963.